Published in final edited form as:
Inorg Chem. 2012 October 15; 51(20): 11017–11029. doi:10.1021/ic301506x.

Synthesis of Binucleating Macrocycles and their Nickel(II) Hydroxo- and Cyano-Bridged Complexes with Divalent Ions: Anatomical Variation of Ligand Features

Xiaofeng Zhang[§], **Deguang Huang**[§], **Yu-Sheng Chen**[†], and **R. H. Holm**[†,*]

[§]Department of Chemistry and Chemical Biology, Harvard University, Cambridge, Massachusetts 02138, United States

[†]Center for Advanced Radiation Source, University of Chicago c/o APS/ANL, Bldg. 434 D, Argonne, IL 60439, United States

Abstract

The planar NNN-pincer complexes $[M^{II}(pyN^{Me}{}_2)(OH)]^{1-}$ (M^{II} = Ni, Cu) fix CO_2 in η^1-OCO_2H complexes; results for the copper system are described. Mn^{II}, Fe^{II}, Co^{II}, and Zn^{II} behave differently, forming $[M^{II}(pyN_2{}^{Me})_2]^{2-}$ with N_4O_2 coordination. Incorporation of the Ni^{II} pincer into binucleating macrocycle **2** containing a triamino M^{II} locus connected by two 1,3-biphenylene groups affords proximal Ni^{II} and M^{II} sites for investigation of the synthesis, structure, and reactivity of Ni-X-M bridge units. This ligand structure is taken as a reference for variations in M^{II} atoms and binding sites and bridges X = OH^- and CN^- to produce additional members of the macrocyclic family with improved properties. Macrocycle **2** with a 22-membered ring is shown to bind M^{II} = Mn, Fe, and Cu with hydroxo bridges. Introduction of the 4-Bu^{i}O group (macrocycle **3**) improves the solubility of neutral complexes such as those with Ni^{II}-OH-Cu^{II} and Ni^{II}-CN-Fe^{II} bridges. The syntheses of macrocycle **5** with a 7-Me-[12]aneSN_3 and macrocycle **6** with a 1,8-Me_2-[14]aneN_4 M^{II} binding site are described to together with hydoxo-bridged Ni-Cu and cyano-bridged Ni-Fe complexes. This work was motivated by the presence of a Ni···(HO)-Fe bridge grouping in a reactive state of carbon monoxide dehydrogenase. Attempted decrease in Ni-(OH)-M distances (3.70-3.87 Å) to smaller values observed in the enzyme by use of macrocycle **4** having 1,2-biphenylene connectors led to a mononuclear octahedral Ni^{II} complex. Bridge structural units are summarized and the structures of fourteen macrocyclic complexes including eight with bridges are described.

INTRODUCTION

The Ni^{II}···(HO)-Fe^{II} bridge grouping is a component of the catalytic site (C-cluster) in the Ni-Fe-S enzyme carbon monooxide dehydrogenase which catalyzes the reaction CO + H_2O ⇌ CO_2 + $2H^+$ + $2e^-$.[1-4] The site consists of a $NiFe_3S_4$ cubanoid cluster to which is bound via a C_3-S atom an exo Fe^{II} atom that is part of the bridge. While the cluster portion has been chemically synthesized,[5,6] attainment of the complete assembly $NiFe_3S_4$-Fe_{exo} has proven elusive. Consequently, more recent research has concentrated on a different approach which departs from a Ni-Fe-S support platform but allows an investigation of the chemistry of Ni^{II} and Fe^{II} in combination. Suitable binucleating macrocyclic ligands allow specific

*Corresponding Author: holm@chemistry.harvard.edu.

ASSOCIATED CONTENT

! Supporting Information. Crystallographic data for 20 compounds (Tables S1-S4), structure of complex **28**, synthesis of macrocycles **3** and **4**, UV-visible spectra of the Ni^{II}-OH compounds **17**, **21** and **26**.

binding of the two metals in bridging juxtaposition at a known distance and variation of the atom or bridging group between them. The dianion of **2** in Figure 1 is a first approach to the problem.[7] The upper NNN site, obviously related to the pincer ligand **1** with two deprotonated amide groups, binds Ni^{II} while the lower triamine portion binds Fe^{II}. Various bridges including hydroxo, formate, and cyano may be interposed between the two metal sites. A further advantage of the system is that the terminal hydroxo pincer complex $[Ni(pyN_2^{Me2})(OH)]^{1-}$, [8] a virtual replica of the binuclear Ni^{II} site, may be prepared and its reactivity examined separately.[9,10] This complex reacts quantitatively and reversibly with CO_2 to afford an η^1-HCO_3 product in an exceptionally fast second-order reaction in DMF ($k_2^{298} \approx 10^6\ M^{-1}s^{-1}$).

We are engaged in producing a new set of macrocycles and their complexes that sustain proximal Ni···M binding with bridge formation and retain the pincer binding site but with otherwise variable and/or improved properties. With attention to the reference macrocyclic complex in Figure 2 which includes hydroxo as a representative bridging group, we note four regions of potential modification. Region I is the site of atom M and associated ligands. Various atoms M and ligands, bridging and terminal (if present), in this region are subject to incorporation dependent on several factors. That of primary interest in ligand design is the binding functionality present in region IV. Introduction of a suitable substituent R in region II would enhance the solubility of neutral complexes such as $[Ni(\mu_2\text{-}OH)FeCl(\subset_{22}\text{-}pyN_2dien^{Me3})]$ (see below), allowing solution studies. Adjustment of the spacer group between binding sites in region III could control the Ni···M separation. Variation of the ligand framework in region IV (M site) might lead to tighter binding of atom M, a problem we have encountered on occasion in this work. Lastly, given the huge number of known binucleating (or "compartmental") ligands,[11-13] it need be recognized that the binuclear complex in Figure 2 and any alterations of it constitute a small subset of possibilities for examination of the chemistry of proximally bound metals. In this report, we demonstrate certain modifications in regions I-IV by synthesis and structure determinations. As will be seen, all modifications are illustrative of further possibilities and all but that in region II allow bridge formation.

EXPERIMENTAL SECTION

Preparation of Compounds

Unless otherwise stated, all reactions and manipulations were performed under a dinitrogen atmosphere. Volume reduction and drying steps were performed in vacuo; filtrations were through Celite. Commercial grade chemicals were used without further purification. Acetonitrile, THF, and diethyl ether were purified by an Innovative Technology or MBraun solvent purification system. DMF was freshly distilled from CaH_2 and dried over molecular sieves for 24 h. Compounds were identified by combinations of elemental analyses, spectroscopic measurements (mainly ^1H NMR where possible), and X-ray structure determinations. Representative compounds were analyzed (Midwest Microlab, Inc.). The structures of the NNN-pincer ligand **1** and binucleating macrocycles **2-6** are provided in Figure 1.

In the sections that follow, ligands and complexes are numerically designated according to Chart 1 and Figures 1, 3-7, 9, 11, 12, and 14.

(1) Complexes Derived from the Pincer Ligand $H_2pyN_2^{Me2}$·$(Et_4N)[Cu(pyN_2^{Mw2})(OH)]$

$H_2pyN_2^{ME2}$ (75 mg, 0.20 mmol)[7] and $Cu(OTf)_2$ (72 mg, 0.20 mmol) were stirred in DMF (3 mL) for 20 min. The light green solution was treated slowly with Et_4NOH (25% in methanol, 353 mg, 0.60 mmol) and the mixture was stirred for 12 h to form a purple-blue

solution and a small amount of sticky precipitate which was removed by filtration. Ether (18 mL) was added to the filtrate resulting in a cloudy suspension from which crystals separated over 3 h. The product was collected as a purple-blue crystalline solid (85 mg, 73%). Absorption spectrum (DMF): λ_{max} (ε_M) 594 (br, 270) nm. IR (KBr): ν_{OH} 3608 cm$^{!1}$. *Anal.* Calcd. for $C_{31}H_{42}CuN_4O_3$: C, 63.95; H, 7.27; N, 9.62. Found: C, 63.85; H, 7.23; N, 9.52.

$(Et_4N)[Cu(pyN_2^{Me2})(HCO_3)]$

A solution of $(Et_4N)[Cu(pyN_2)(OH)]$ (29 mg, 0.050 mmol) in DMF (3 mL) was bubbled with carbon dioxide for 15 min. Diffusion of ether into the blue solution afforded the product as blue crystals (25 mg, 80%). Absorption spectrum (DMF): λ_{max} (ε_M) 610 (br, 320) nm.

$(Et_4N)_2[Fe(pyN_2^{Me2})_2]$

A solution of H_2pyN_2 (112 mg, 0.30 mmol) in DMF (3 mL) was treated with NaH (15 mg, 0.060 mmol) slowly to give a light yellow solution, to which was added $Fe(OTf)_2$ (106 mg, 0.30 mmol). The dark purple reaction mixture was stirred for 2 h and filtered. Ether (20 mL) was added to the filtrate causing separation of a purple oil, which was treated with ether to form a purple solid. The solid was dissolved in THF (5 mL) and solution was filtered through Celite to give a deep purple solution. A solution of Et_4NOH (25% in methanol, 176 mg, 0.30 mmol) was slowly added, and the mixture was stirred for 2 h and filtered to remove a sticky white precipitate. Ether (15 mL) was added to the filtrate to form a blue solid, which was dissolved in DMF (2 mL). Addition of ether by diffusion caused separation of the product as blue-red crystals (71 mg, 45%). *Anal.* Calcd. for $C_{62}H_{82}FeN_8O_4$: C, 70.30; H, 7.80; N, 10.58. Found: C, 70.19; H, 7.83; N, 10.66.

$(Et_4N)_2[Co(pyN_2^{Me2})_2]$

A mixture of H_2pyN_2 (75 mg, 0.20 mmol) and $Co(OTf)_2$ (71 mg, 0.20 mmol) in DMF was stirred for 30 min. The pink-red solution was slowly treated with a solution of Et_4NOH (25% in methanol, 353 mg, 0.60 mmol) and the reaction mixture was stirred for 6 h to form a red solution and a sticky precipitate, which as removed by filtration through Celite. Ether (15 mL) was added to the filtrate causing formation of a red oil. Addition of ether to the oil formed a red solid, which was washed with THF (5 mL) and dissolved in DMF (2 mL). Diffusion of ether into the solution afforded the product as violet block-like crystals (53 mg, 50%). *Anal.* Calcd. for $C_{62}H_{82}CoN_8O_4$: C, 70.10; H, 7.78; N, 10.55. Found: C, 69.92; H, 7.92; N, 10.66.

$(Et_4N)_2[Mn(pyN_2^{Me2})_2]$

The preceding method was followed with use of $Mn(OTf)_2$ (71 mg, 0.20 mmol) and gave the product as a yellow crystalline solid (70 mg, 66%). *Anal.* Calcd. for $C_{62}H_{82}MnN_8O_4$: C, 70.36; H, 7.81; N, 10.59. Found: C, 70.04; H, 7.87; N, 10.46.

$(Et_4N)_2[Zn(pyN_2^{Me2})_2]$

The preceding method was followed with use of $Zn(OTf)_2$ (73 mg, 0.20 mmol) and gave the product as a yellow crystalline solid (77 mg, 72%). *Anal.* Calcd. for $C_{62}H_{82}N_8O_4Zn$: C, 69.68; H, 7.73; N, 10.48. Found: C, 69.51; H, 7.91; N, 10.52

(2) Binuclear Complexes Derived from Macrocycle $\subset_{22}$-$H_2pyN_2dien^{Me3}$

Macrocycle **2** and complexes **13** and **15** were prepared as described.[7]

[Ni(μ$_2$-OH)MnCl(⊂$_{22}$-pyN_2^{Me3})]

To a solution of (Et_4N)[Ni(OH)(⊂$_{22}$-pyN_2dien^{Me3})] (28 mg, 0.040 mmol) in DMF (2 mL) was added a solution of $MnCl_2$ (5.0 mg, 0.040 mmol) in DMF (1 mL). The reaction mixture was stirred for 1 h, filtered, and ether was diffused into the deep red filtrate for 2 d. The solid was washed with acetonitrile (3 mL) and dried to afford the product as red crystals (11 mg, 42%). *Anal.* Calcd. for $C_{28}H_{33}ClMnN_6NiO_3$: C, 51.68; H, 5.11; N, 12.92. Found: C, 51.62; H, 5.18; N, 13.01.

[Ni(μ$_2$-OH)CuCl(⊂$_{22}$-pyN_2dien^{Me3})]

To a solution of (Et_4N)[Ni(OH)(⊂$_{22}$-pyN_2dien^{Me3})] (21 mg, 0.030 mmol) in DMF (2 mL) was added a solution of $CuCl_2$ (4.1 mg, 0.030 mmol) in DMF (1 mL). The reaction mixture was stirred for 30 min, filtered, and ether was diffused into the brown-red filtrate to form a solid. This material was washed with acetonitrile (3 mL) and dried in vacuo to give the product as orange-yellow crystals (8.0 mg, 41%).

(3) Complexes Derived from Macrocycle ⊂$_{22}$-4-Bu^{i}O-H$_2$pyN_2dien^{Me3}

The five-step synthesis of macrocycle **3**, obtained in 16% overall yield based on chelidamic acid, is given elsewhere.[14]

(Me_4N)[Ni(OH)((⊂$_{22}$-4-Bu^{i}O-pyN_2dien^{Me3})]

Macrocycle **3** (56 mg, 0.10 mmol) and Ni(OTf)$_2$ (37 mg, 0.10 mmol) were mixed and stirred in DMF (2 mL) for 15 min to give a light yellow suspension. Me_4NOH (25% in methanol, 55 mg, 0.015 mmol) was added and the mixture was stirred for 1 h, forming a red suspension. A second equal portion of Me_4NOH was added and the mixture was stirred for 4 h to give a deep red solution with some sticky precipitate which was removed by filtration. Addition of ether (40 mL) to the filtrate deposited an orange-red material, which was dissolved in DMF/THF (6 mL, 1/5 v/v) to give a red solution. Ether (5 mL) was added and a white solid was filtered off. A second portion of ether (10 mL) was added and the solution was stored overnight, resulting in the separation of a red crystalline solid (31 mg, 44%). Absorption spectrum (DMF): λ_{max} (ε_M) 400 (5460) nm. IR (KBr): ν_{OH} 3608 cm^{-1}. ^{1}H NMR (DMF-d_7): δ −4.71 (s, 1), 1.03 (d, 6), 2.05 (s, 3), 2.10 (m, 1), 2.18 (m, 4), 2.26 (m, 4), 2.28 (s, 6), 3.35 (s, 4), 3.99 (d, 2), 6.79 (d, 2), 7.04 (m, 4), 7.18 (s, 2), 7.25 (d, 2). *Anal.* Calcd. for $C_{36}H_{53}N_7NiO_4$: C, 61.20; H, 7.56; N, 13.88. Found: C, 60.29, H, 7.70; N, 14.02.

[Ni(μ$_2$-OH)CuCl(⊂$_{22}$-4-Bu^{i}O-pyN_2dien^{Me3})]·DMF

$CuCl_2$ (4.0 mg, 0.030 mmol) in DMF (0.5 mL) was added dropwise to a solution of (Me_4N)[Ni(OH)(⊂$_{22}$-4-Bu^{i}O-pyN_2-dien^{Me3})] (21 mg, 0.030 mmol) in DMF (2 mL). The reaction mixture was stirred for 1 h and filtered. Diffusion of ether into the filtrate deposited the product as tea-brown block-like crystals (15 mg, 62%). IR (KBr): ν_{OH} 3557 cm^{-1}. *Anal.* Calcd. for $C_{35}H_{48}ClCuN_7NiO_5$: C, 52.25; H, 6.01; N, 12.19. Found: C, 51.91; H, 5.90; N, 11.97.

[Ni(μ$_2$-CN)FeCl(⊂$_{22}$-4-Bu^{i}O-pyN_2dien^{Me3})]·½Et_2O

A mixture of (Me_4N)-[Ni(OH)(⊂$_{22}$-4-Bu^{i}O-pyN_2dien^{Me3})] (35 mg, 0.050 mmol) and Et_4NCN (9.4 mg, 0.060 mmol) was stirred in DMF (3 mL) for 3 h and filtered. $FeCl_2$ (6.3 mg, 0.050 mmol) in DMF (0.5 mL) was added to the orange-red filtrate. The mixture was stirred for 1 hr, filtered, and ether (18 mL) was added slowly to the filtrate to deposit a white precipitate, which was filtered off. Ether was diffused into the filtrate, causing separation of a red crystalline solid. This material was dissolved in 4 mL of DMF/propionitrile (1:1 v/v) and diffused with ether to deposit the product as orange-red crystals (17 mg, 44%). IR: ν_{CN}

2117 $cm^{!1}$. *Anal.* Calcd. for $C_{35}H_{45}ClFeN_7NiO_{3.5}$: C, 54.61; H, 5.89; N, 12.74. Found: C, 54.59; H, 5.85; N, 12.80.

(4) Ni^{II} Complex Derived from Macrocycle $\subset_{20}$-$H_2pyN_2dien^{Me3}$

The preparation of macrocycle **4** (25% overall yield based on *o*/nitrobenzaldehyde) is described elswhere.[14]

[Ni($\subset_{20}$-pyN_2dien^{Me3})]

Macrocycle **4** (97 mg, 0.20 mmol) and $Ni(OTf)_2$ (71 mg, 0.20 mmol) were reacted in DMF/THF (5 mL, 3:2 v/v) for 1 h to give a light yellow suspension. Et_4NOH (25% in methanol, 118 mg, 0.20 mmol) was added and the reaction mixture was stirred for 1 h forming a light green suspension. A second equal portion of Et_4NOH was added and the mixture was stirred for 10 h to give a green solution and a white precipitate, which was removed by filtration. Ether (20 mL) was added to the filtrate, forming a green oil. The mixture was allowed to stand overnight, yielding the product as a green crystalline solid (43 mg, 40%).

(5) Macrocylic Ligand $\subset$-$H_2pyN_2SN_3^{Me}$ and Complexes

The synthesis of macrocycle **5** (11% overall yield based on **5a**) is given in Figure 3.

(a) Intermediates 5a-5e

To a mixture of thioglycollic acid (21.0 g, 0.140 mol) in thionyl chloride (45 mL) was added 0.15 mL of dry DMF as a catalyst. The mixture was stirred for 4 h at 45EC to give a clear orange solution. Excess thionyl chloride was partially removed to leave a red-black solution from which pure **5a**[15] was obtained by distillation (130E/3.0 mm Hg). Solutions of **5a** (2.80 g, 15.0 mmol) and 3-*N*-methylaminopentane-1,5-diamine (3.51 g, 30.0 mmol), each in dry toluene (40 mL), were added simultaneously to chloroform (500 mL) by syringe pump over 16 h. After removal of a white precipitate and evaporation of the filtrate, the yellow-orange solid was purified on a silica column eluted with CH_2Cl_2/MeOH/NH_4OH (300/80/1 v/v) to yield **5b** as a white solid (1.80 g, 52%). ^1H NMR ($CDCl_3$): δ 2.30 (s, 3), 2.48 (t, 4), 3.24 (s, 4), 3.30 (q, 4), 7.26 (s, 2). ESMS: m/z 232 $(M+H)^+$.

To a suspension of **5b** (1.80 g, 7.8 mmol) in dry THF (20 mL) was added a solution of Me_2SBH_3 (16 mL, 32 mmol). The mixture was refluxed at 75EC for 5 h. Methanol was added to the white slurry, the mixture was stirred for 1 h, and the solvent was removed to leave a foam-like residue. This material was refluxed in 6 M aqueous HCl (35 mL) for 3 h and solvent was removed to give a white solid, which was treated with 2 M aqueous NaOH until pH ~14 was reached. The mixture was extracted with chloroform (5 × 70 mL), the combined organic layers were dried ($MgSO_4$), and solvent was removed to leave **5c** as a colorless crystalline solid (0.95 g, 60%). ^1H NMR ($CDCl_3$): δ 2.17 (s, 3), 2.37 (t, 4), 2.55 (q, 8), 2.63 (t, 4), 2.68 (br, s, 2).

A mixture of *N*-(*tert*-butoxycarbonyl)-3-bromomethylaniline[16] (1.35 g, 4.72 mmol), **5c** (0.48 g, 2.36 mmol), K_2CO_3 (0.65 g, 4.72 mmol), and KI (0.39 g, 2.36 mmol) was refluxed in acetonitrile (200 mL) for 36 h, the mixture was filtered, and the solvent evaporated to leave a light yellow solid residue. This material was dissolved in dichloromethane (100 mL), the solution was filtered, and the solvent removed. The residue was purified on a silica column eluted with CH_2Cl_2/MeOH/NH_4OH (70/8/5 v/v) to yield **5d** as a white foam-like solid (1.04 g, 72%). ^1H NMR ($CDCl_3$): δ 1.53 (s, 18), 2.11 (s, 3), 2.45 (s, 4), 2.54 (s, 4), 2.76 (t, 4), 2.98 (t, 4), 3.59 (s, 4), 6.67 (s, 2), 7.05 (d, 2), 7.23 (t, 2), 7.30 (d, 2), 7.35 (s, 2). ESMS: m/z 614 $(M+H)^+$.

To a solution of **5d** (1.04 g, 1.70 mmol) in dichloromethane (10 mL) was added trifluoroacetic acid (3 mL); the mixture was stirred for 2 h. The orange-red mixture was added slowly to a 2 M aqueous NaOH solution (50 mL), stirred for 20 min, and diluted with water (20 mL). The organic layer was collected and the aqueous layer was extracted with dichloromethane. The combined organic layers were washed with brine (2 × 70 mL) and dried ($MgSO_4$). Solvent was removed to afford **5e** as a pale yellow oil (0.674 g, 96%). ^{1}H NMR ($CDCl_3$): δ 2.12 (s, 3), 2.48 (s, 4), 2.55 (s, 4), 2.76 (t, 4), 2.96 (t, 4), 3.53 (s, 4), 3.66 (s, 4), 6.56 (d, 2), 6.71-6.74 (m, 4), 7.08 (t, 2).

(b) Macrocycle ⊂-$H_2pyN_2SN_3^{Me}$)]

To a solution of Et_3N (6.0 mL) in dry THF (350 mL) was added simultaneously solutions of pyridine-2,6-dicarbonylchloride (0.365 g, 1.79 mmol) in THF (50 mL) and **5e** (0.674 g, 1.63 mmol) in THF/acetonitrile (50 mL, 4/1 v/v) by syringe pump over 20 h. The mixture was filtered and solvent was evaporated to give a yellow-brown solid, which was dissolved in dichloromethane (7 mL). Upon standing for several h, the solution deposited a colorless crystalline solid which was collected and washed with dichloromethane (2 × 3 mL). The solid was dissolved in dichloromethane/methanol (8/2 mL) and dried to give the macrocyclic **5** as a white powder (0.47 g, 53%). ^{1}H NMR (Me_2SO-d_6): δ 2.53 (m, 2), 2.65-2.73 (m, 7), 2.75-2.87 (m, 6), 3.21 (m, 2), 3.64 (s, 4), 3.70 (m, 2), 7.05 (d, 2), 7.37 (t, 2), 7.53 (s, 2), 8.32 (t, 1), 8.39 (m, 4), 11.14 (s, 2). ESMS: m/z 545 $(M+H)^+$.

(c) Complexes. (Me_4N)[Ni(OH)(⊂-$pyN_2SN_3^{Me}$)]

Macrocycle **5** (82 mg, 0.15 mmol) and $Ni(OTf)_2$ (54 mg, 0.15 mmol) were stirred in DMF (3 mL) for 12 h to give a light yellow suspension. Me_4NOH (25% in methanol, 82 mg, 0.15 mmol) was added dropwise and the mixture was stirred for 4 h. An equal portion of Me_4NOH was added, the mixture was stirred for 4 h, and was filtered to remove a sticky precipitate. Ether was added to the filtrate to deposit an orange-red solid that was collected and washed with ether (3 mL). The solid was dissolved in DMF (7 mL) and filtered. The red filtrate was diffused with ether to cause separation of a red solid together with some white precipitate. The red product was separated manually and dried (52 mg, 50%). Absorption spectrum (DMF): λ_{max} (ε_M) 412 (5500), 488 (sh, 1800) nm. IR (KBr): ν_{OH} 3601 cm!1. ^{1}H NMR (DMF-d_7): δ −4.20 (s, 1), 1.94 (m, 2) 2.12 (s, 3), 2.41 (m, 2), 2.56 (m, 4), 2.80 (m, 2), 2.87 (m, 2), 2.98 (m, 4), 3.48 (d, 2), 3.59 (d, 2), 6.73 (d, 2), 6.98 (t, 2), 7.27 (d, 2), 7.52 (d, 2), 7.67 (s, 2), 8.05 (t, 1). *Anal.* Calcd. for $C_{34}H_{47}N_7NiO_3S$: C, 58.97; H, 6.84; N, 14.16. Found: C, 59.02; H, 6.79; N, 13.97.

[$Ni(OH_2)$(⊂-$pyN_2SN_3^{Me}$)]

A solution of (Me_4N)[Ni(OH)(⊂-$pyN_2SN_3^{Me}$)] (21 mg, 0.03 mmol) was added to solid NH_4HCO_3 (4.7 mg, 0.06 mmol). The mixture was stirred for 3 h and filtered. The filtrate was diffused with ether to precipitate some colorless crystals which were removed by filtration. The red filtrate was reduced to a red oily solid, which was dissolved in THF (0.5 mL). The solution was diffused with ether to deposit a red microcrystalline product (8.0 mg, 43%) which was identified by an X-ray structure determination.

[NiClFeCl(⊂-$pyN_2SN_3^{Me}$)]

$FeCl_2$ (3.8 mg, 0.030 mmol) in DMF (0.5 mL) was added dropwise to a red solution of (Me_4N)[Ni(OH)(⊂-$pyN_2SN_3^{Me}$)] (21 mg, 0.030 mmol) in DMF (3 mL). The reaction mixture was stirred for 2 h and filtered to remove some black precipitate. A second equal portion of $FeCl_2$ in DMF (0.5 mL) was added slowly to the red-brown filtrate. The mixture was stirred for 2 h and filtered. Diffusion of ether into the filtrate afforded the red crystalline product (10 mg, 41%).

[Ni(μ$_2$-CN)FeCl(⊂-py$N_2SN_3^{Me}$)]·Me_2SO

A mixture of (Me_4N)[Ni(OH)(⊂-py$N_2SN_3^{Me}$)] (21 mg, 0.030 mmol) and Et_4NCN (5.6 mg, 0.036 mmol) was stirred in DMF (2 mL) for 5 h and filtered. Ether was added to deposit a red solid, which was washed with THF/ether (3 mL, 2:1 v/v) and dissolved in DMF (1 mL). $FeCl_2$ (3.8 mg, 0.030 mmol) in DMF (0.5 mL) was added slowly to the red solution, which was stirred for 1 h and filtered. Ether (20 mL) was added to the filtrate to obtain a red solid which was washed with ether (1 mL) and acetonitrile (1 mL). The red solid was dissolved in Me_2SO (1 mL) and the solution was layered with ethyl acetate to cause separation of a red crystalline solid and a white precipitate. The red solid was manually separated and dried to yield the product (11 mg, 46%). IR: ν_{CN} 2137 cm^{-1}.

[Ni(μ$_2$-OH)Cu(⊂-py$N_2SN_3^{Me}$)](ClO_4)

A solution of (Me_4N)[Ni(OH)(⊂-py$N_2SN_3^{Me}$)] (21 mg, 0.030 mmol) in DMF (2.5 mL) was added quickly to a solution of $Cu(ClO_4)_2·6H_2O$ (11 mg, 0.030 mmol) in DMF (0.5 mL). The mixture was stirred for 10 min and filtered. The filtrate was diffused with ether causing the product to separate as a black-green crystalline solid (14 mg, 60%). IR (KBr): ν_{OH} 3516 cm^{-1}. *Anal.* Calcd. for $C_{30}H_{35}ClCuN_6NiO_7S$: C, 46.11; H, 4.51; N, 10.76. Found: C, 45.93; H, 4.47; N, 10.54.

(6) Macrocyclic Ligand ⊂-H_2py$N_2N_4^{Me2}$ and Complexes

The synthetic route to macrocycle **6** (10% overall yield based on **6a**) is provided in Figure 4.

(a) Intermediates 6a-6c

Compound **6a** has been previously used but no preparation was reported.[17] PPh_3 (4.72 g, 18.0 mmol) was added to a solution of 2-[(3-hydroxymethyl)phenyl]isoindoline-1,3-dione[18] (3.04 g, 12.0 mmol) in dichoromethane (30 mL). The mixture was cooled to −5EC and CBr_4 (5.97 g, 18.0 mmol) in dichloromethane (30 mL) was added dropwise. The mixture was stirred at −5EC for 2 h and allowed to warm to room temperature. Ethyl acetate (150 mL) was added and the solution was washed with brine (4 × 70 mL). The organic layers were combined and dried over $MgSO_4$, and solvent was removed to leave a light yellow-brown residue. The crude product was purified on a silica column eluted with dichloromethane/hexanes (1:1 v/v) to give **6a** as a white solid (3.21 g, 85%). ^{1}H NMR ($CDCl_3$): δ 4.54 (s, 2), 7.42 (m, 2), 7.50 (m, 2), 7.81 (m, 2), 7.96 (m, 2). ESMS: m/z 338 $(M + Na)^+$.

Compound **6a** (2.71 g, 8.60 mmol), 1,8-dimethyl-1,4,8,11-tetraazacyclotetradecane (1,8-Me_2-[14]aneN_4) (0.98 g, 4.3 mmol), K_2CO_3 (1.19 g, 8.60 mmol), and KI (0.71 g, 4.3 mmol) were refluxed in acetonitrile (300 mL) for 60 h. The mixture was filtered and solvent was removed to leave a light brown solid. This material was purified on a silica column eluted with dichloromethane/methanol/NH_4OH to give **6b** as a pale yellow solid (0.96 g, 32%). ^{1}H NMR ($CDCl_3$): δ 1.64 (m, 4), 2.11 (s, 6), 2.46 (m, 8), 2.58 (m, 8), 3.61 (s, 4), 7.27 (d, 2), 7.41 (m, 6), 7.78 (m, 4), 7.94 (m, 4). ESMS: m/z 699 $(M + H)^+$, 350 $(M + 2H)^{2+}/2$.

To a hot solution of **6b** (0.96 g, 1.38 mmol) in 30 mL of THF and 10 mL of ethanol was added $N_2H_4·H_2O$ (1.0 g, 20 mmol). The mixture was refluxed at 80EC for 15 h to give a white suspension. Ethanol (50 mL) was added and the mixture was filtered. Solvent removal gave a pale yellow oil. The product was purified on a silica gel column eluted with dichloromethane/methanol/NH_4OH (15/3/2 v/v) give **6c** as a colorless oily solid (453 mg, 75%). ^{1}H NMR ($CDCl_3$): δ 1.67 (m, 4), 2.14 (s, 6), 2.49 (m, 8), 2.57 (m, 8), 3.46 (s, 4), 3.67 (br s, 4), 6.55 (d, 2), 6.70 (m, 4), 7.06 (t, 2). ESMS: m/z 439 $(M + H)^+$.

(b) Macrocycle ⊂-$H_2pyN_2N_4^{Me2}$

To a solution of Et_3N (5.5 mL) in dry THF (300 mL) was added simultaneously solutions of pyridine-2,6-dicarbonylchloride (0.245 g, 1.20 mmol) in THF (40 mL) and **6c** (0.44 g, 1.00 mmol) in THF/acetonitrile (40 mL, 3:1 v/v) by syringe pump over 20 h. The mixture was filtered and the solvent removed to leave a light yellow solid. The crude product was purified on a silica column eluted with dichloromethane/methanol/NH_4OH (60/6/1 v/v) to afford the macrocycle **6** as a while powder (285 mg, 50%). ^1H NMR ($CDCl_3$): δ 1.70 (m, 2), 1.77 (m, 2), 2.13 (s, 6), 2.21 (m, 6), 2.45 (m, 4), 2.62 (m, 2), 2.92 (m, 2), 3.16 (m, 2), 3.47 (m, 2), 3.74 (m, 2), 6.97 (d, 2), 7.35 (t, 2), 7.44 (s, 2), 8.15 (t, 1) 8.47 (d, 2), 8.56 (d, 2), 9.61 (s, 2). ESMS: m/z 570 $(M + H)^+$, $(M + 2H)^{2+}/2$.

(c) Complexes. $(Me_4N)[Ni(OH)(⊂\text{-}pyN_2N_4^{Me2})]\cdot½Et_2O$

$Ni(OTf)_2$ (36 mg, 0.10 mmol) in DMF/THF (4 mL, 3:1 v/v) was stirred for 12 h to give a light yellow suspension. Macrocycle **6** (57 mg, 0.10 mmol) was added, followed by dropwise addition of Me_4NOH (25% in methanol, 55 mg, 0.15 mmol). The mixture was stirred for 2 h, a second equal portion of Me_4NOH was introduced, and stirring was continued for 4 h. The mixture was filtered to remove a sticky precipitate, and ether (20 mL) was added to the filtrate. The orange solid that separated was washed with ether (3 mL), dissolved in DMF (2 mL), and THF (2 mL) was added. The solution was filtered and the filtrate diffused with ether to give a mixture of red and white solids. This was washed with THF (1 mL) and DMF (0.5 mL) to afford the product as red plate-like crystals (35 mg, 46%). Absorption spectrum (DMF): λ_{max} (ε_M) 412 (5350), 488 (sh, 1800) nm. IR (KBr): ν_{OH} 3603 $cm^{!1}$. ^1H NMR (DMF-d_7): δ −4.15 (s, 2), 1.45 (m, 2), 1.61 (m, 2), 2.02 (s, 6), 2.07 (m, 2), 2.18 (m, 2), 2.31 (m, 2), 2.42 (t, 4), 2.69 (m, 2), 2.82 (m, 2), 2.99 (m, 2), 3.22 (m, 2), 3.50 (m, 2), 6.72 (d, 2), 6.97 (t, 2), 7.26 (d, 2), 7.52 (m, 4), 8.04 (t, 1). *Anal.* Calcd. for $C_{39}H_{59}N_8NiO_{3.5}$: C, 62.07; H, 7.88; N, 14.85. Found: C, 62.16; H, 7.91; N, 14.45.

$[Ni(\mu_2\text{-}OH)(DMF)_2Cu(⊂\text{-}pyN_2N_4^{Me2})](ClO_4)$

The preceding compound was recystallized from DMF/THF/$C_6H_5CF_3$ (1:10:25 v/v) to give the product in essentially quantitative yield as a green-black crystalline solid. The compound was identified by an X-ray structure determination.

X-ray Structure Determinations

Twenty of the compounds in Chart 1 were structurally characterized; for brevity, compounds that are salts are referred to by their cation or anion number. Diffraction-quality crystals were obtained from the following solvents: dichloromethane/ether/hexane, **4**; DMF/acetonitrile/ether, **5**; methanol/chloroform/ethyl acetate, **6**; DMF/ether, **7**, **8**, **11**, **14**, **16**, **18**, **20**, **21**, **23**, **25-27**; DMF/toluene/ether, **17**, **22**; DMF/propionitrile/ether, **19**; Me_2SO/ethyl acetate, **24**; DMF/THF/$PhCF_3$, **28**. Diffraction data for **16** (15 K) and **22** (95 K) were obtained using synchrotron radiation at the Advanced Photon Source (APS), Argonne National Laboratory. Intensities of reflections were collected by means of a Bruker APEX II CCD together with the D8 Diffractometer equipped with an Oxford Cryosystems helium/nitrogen open flow apparatus. The collection method involved 0.5E scans in φ at −5E in 2q. Other diffraction data were collected with a Bruker CCD area detector diffractometer equipped with an Oxford 700 low-temperature nitrogen apparatus (100 K). Data integration was carried out using SAINT V7.46A with reflection size optimization, and absorption corrections made with SADABS (*Bruker AXS APEX II*, Bruker AXS Inc., Madison, WI 53711). Structures were solved by direct methods using the SHELX program package. All non-hydrogen atoms were refined anisotropically and the temperature factors of those disordered atoms were restrained by DELU/SIMU to achieve an anisotropic average. Hydrogen atoms were not added to the cations (**7**, **11**) or solvate molecules (**6**, **23**) owing to

highly disordered carbon atoms. The hydrogen atom(s) of −OH groups (**7**, **17**, **18**, **28**) and the $-HCO_3$ group (**8**) were located geometrically. Hydrogen atoms of other −OH groups (**14**, **16**, **18**, **22**, **25-27**) were located from difference Fourier maps and refined isotropically. Crystal data and refinement details area given in Tables S1-S4.[14] Other refinement details and explanations (wherever necessary) are included in individual CIF files.

The compounds $(Et_4N)_2[M(pyN_2^{Me2})_2]$ with M = Fe, Mn, and Zn yielded the following crystal data. M = Fe (**10**): triclinic, a = 15.529(3) Å, b = 25.509(5) Å, c = 31.076(6) Å, α = 65.966(4)E, β = 89.778(5)E, γ = 89.945(5)E, V = 11243(4) Å^3, Z = 8, P-1; M = Mn (**9**): triclinic, a = 10.4628(4) Å, b = 16.2333(6) Å, c = 18.9633(7) Å, α = 78.432(1)E, β = 80.522(1)E, γ = 83.378(1)E, V = 3100.9(2), Z = 2, P-1; M = Zn (**12**): orthorhombic, a = 12.723(5) Å, b = 28.53(1) Å, c = 15,467(6) Å, V = 5614(9), Z = 4, *Pbcn*. Sufficient data were collected to show that **9** and **10** have the same structure as **11** in its Et_4N^+ salt. Complex **12** is assigned the structure of **11** based on crystal isomorphism.

The metal contents in selected binuclear complexes were determined at the APS by multiple wavelength anomalous dispersion techniques.[14] The following electron densities normalized to one metal atom per molecule were determined and Ni:M atom ratios calculated: **19** – Ni 0.967(3), Fe 0.961(3), 1.01:1; **24** – Ni 0.938(5), Fe 0.851(5), 1.10:1; [**25**](ClO_4) – Ni 1.000(5), Cu 0.964(5), 1.04:l; [**28**](ClO_4) – Ni 0.968(5), Cu 0.953(3), 1.02:1.

RESULTS AND DISCUSSION

Pincer Complexes with Other Metals. (a) Cu^{II}

Prior to pursuing ligand alterations in regions I-IV of the complex in Figure 2, we wished to know what other divalent metals might bind in the NNN pincer site. Such metals would be candidates for incorporation into binucleating macrocycles containing that site and also may engage in CO_2 fixation. To do so, we utilized for simplicity ligand **1**. The planar complexes $[M(pyN_2^{Me2})(OH)]^{1-}$ (M = Ni^{II}, Pd^{II}) have been previously described. Both react cleanly with CO to afford $[M(pyN_2^{Me2})(HCO_3)]^{1-}$ in good yield. The corresponding Cu^{II}-OH complex **7** is easily prepared by the reaction of $Cu(OTf)_2$ and Et_4NOH in DMF. It reacts immediately with CO_2 in DMF to form the η^1-HCO_3 complex **8** which is isolable in 80% yield. The spectrophotometric conversion **7** → **8** is illustrated with Figure 5 together with the planar structures and selected dimensions of the two complexes which are isostructural with their Ni^{II} and Pd^{II} counterparts, and nearly isometric with the Ni^{II} complex. Mononuclear Cu^{II}-OH complexes in different coordination environments have been described.[19-21] However, nearly all Cu^{II}-mediated CO_2 fixation reactions have been carried out with polynuclear bridged oxo and hydroxo reactants and afford carbonate-bridged products.[22-25] Only one four-coordinate η^1-bicarbonate complex, also a pincer species, has been previously characterized.[26,27] It and **8** crystallize as centrosymmetric hydrogen-bonded dimers. The long Cu-O4 distance of 2.542 Å is consistent with a four-coordinate description of **8**. Evidently, the system in Figure 5 is the simplest yet devised for CO_2 fixation by a Cu^{II} reactant.

(b) Mn^{II}, Fe^{II}, Co^{II}, and Zn^{II}

To seek a broader set of reactants, we have examined the reaction of other divalent metals with equimolar $H_2pyN_2^{Me2}$. The results with four divalent ions are summarized in Figure 6, from which it is evident that despite the 1:1 reaction stoichiometry six-coordinate bis-ligand complexes **9-12** are formed. Because of ligand steric factors, these isostructural complexes adopt a MN_4O_2 coordination unit in which one *N*≠substituent of each ligand is rotated in order to place two oxygen atoms mutually *cis*, thus reducing destabilizing steric interactions between *N*-substituents. The structure of **11** (Figure 6) reveals a C_2-symmetric configuration

far removed from octahedral with approximately *cis* oxygen atoms and *trans* O/N-Co-N angles much smaller than 180E. This situation arises because, unlike low-spin d^8 and d^9, the other four metal ions do not have an intrinsic planar stereochemical preference based on *d*-orbital energetics. Further, the pyN_2^{Me2} ligand dianion does not engender bond angles in the usual tetrahedral range. This type of coordination isomerism has several precedents among 2,6-pyridinedicarboxamido complexes.[28-32] These four metal ions are unsuitable for coordination in the pincer site of a macrocycle such as that in Figure 2, but are candidates for binding in the other site.

Modifications in Complexes of Binucleating Ligands

This phase of our work on complexes of binucleating ligands is focused on synthesis and structure proofs by X-ray methods. Physical properties will be described subsequently as needed in reactivity studies. Displayed in Figure 2 is the reference molecule subject to modification. The changes that follow are illustrative of a much broader set of potential alterations. Yields of isolated compounds are indicated. For example, variation in divalent M is confined to Mn^{II}, Fe^{II}, and Cu^{II} and bridging ligands to hydroxo and cyano, although other M atoms and bridges are surely possible. Cyanide was employed to determine if macrocycle flexibility would accommodate a two-atom bridge Ni^{II}-CN-M^{II} approaching linearity. Further, cyanide is an inhibitor of CODH. The X-ray structures of macrocycles **4-6** and complexes **14** and **16-28** were determined; those of macrocycle **2** and complexes **13** and **15** were described earlier.[7] Metric features of bridge units are collected in Table 1; other structural information is available in figure legends and elsewhere.[14] All complexes except **27** and **28** contain planar Ni^{II} coordinated by the NNN pincer ligand. Parameters of the NiN_3 unit are nearly identical across the set **13-26**; data for **17** and **26** are included in Figures 10 and 15, respectively. Stereochemistry at five-coordinate M sites is approximated in terms of the shape parameter $\tau = (\alpha - \beta)/60$ where α and β are largest and next-largest bond angles, respectively.[33] For idealized square pyramidal (SP) $\tau = 0$ and for trigonal bipyramidal (TBP) $\tau = 1$. Note that for four binuclear complexes, mixed metal contents were determined directly by anomalous dispersion methods.

(a) Region I

Different metals are incorporated by binding in the vacant site of mononuclear Ni^{II}-OH complexes **13**, **17**, **21**, and **26**. These precursors are readily prepared and are recognized by upfield −OH resonances at −4.1 to −4.7 ppm (DMF). As shown in Figure 7, different metals M = Mn^{II} (**14**) and Cu^{II} (**16**) can be readily inserted into the vacant triamine site of terminal hydroxo complex **13** in *ca.* 40% yield by reaction with metal chlorides in DMF. The Fe^{II} complex **15**, the first binuclear complex of macrocyle **2**,[7] is included for comparison. The M sites are five-coordinate with intermediate shapes ($\tau = 0.52$ for **14** and 0.50 for **15**), and approach TBP with **16** ($\tau = 0.78$). Complexes **19** (44%, Figure 9) and **23** (46%, Figure 12) containing the Ni^{II}-CN-M^{II} bridge were obtained by cyanide displacement of hydroxo.

(b) Region II

Neutral complexes **14-16** are insoluble or sparingly soluble in organic solvents such as DMF and acetonitrile; as such they are not amenable to studies of solution properties and reactivity. We find that substitution of an isobutoxy group in the 4-position of the pyridine ring affords complexes that are freely soluble in DMF and soluble (but less so) in acetonitrile. These complexes are derived from macrocycle **3** which is accessible by five steps in 16% overall yield from chelidamic acid.[14] Two complexes, hydroxo-bridged **18** (M = Cu^{II}, 62%) and cyano-bridged **19** (M = Fe^{II}, 44%) were prepared from **17** as indicated in Figure 9. Structures are set out in Figure 10. The bridge structural parameters of **18** are similar to those of the Ni/Cu complex **16** except for the Ni···Cu separation which is 0.17 Å

shorter. The Cu^{II} site does not approach the TBP shape of **16**. Instead, the site reveals a highly irregular four-coordinate CuN_2OCl unit with a NNCu/CuOCl dihedral angle of 38.6E and a non-bonded Cu-N4 distance of 2.702(3) Å. This arrangement apparently influences the metal-metal distances, but why substitution at the remote 4-position of the pyridyl ring affects structure is unclear. The DMF solvate molecule[14] does not interact with this site. Cyanide can be readily interposed in the macrocyclic structure **19**, affording nearly linear Ni-C-N (170E) and bent C-N-Fe (138E) bridge segments and an increase of nearly 1.0 Å in metal-metal distance. The Fe^{II} site approaches SP coordination ($\tau = 0.16$) with chloride in the apical position. Thus the reference macrocycle can stabilize two-atom bridges.

(c) Region III

Inasmuch as the Ni···Fe separation in active and cyanide-inhibited CODH is less than 3.0 Å,[1,4,34] we wished to decrease the Ni···M distance in the reference macrocycle. This is most readily accomplished synthetically by changing the two connecting phenylene rings from 1,3− to 1,2−substitution. Macrocycle **4** differs from **2** and **3** by having 20 rather than 22 atoms in its inner ring. Relevant information is provided in Figure 11, which includes a structure proof of the macrocycle. Reaction of **4** with $Ni(OTf)_2$ and base leads to the green distorted octahedral complex **20** (40%) instead of a complex with an Ni^{II}-OH group and a vacant triamine locus. While the pincer site is retained, the smaller ring and the proclivity of Ni^{II} for octahedral coordination favor the observed product. In this context, we note that another NNN pincer macrocycle with a 20-membered ring and a potential pyridyldiamino binding site forms a distorted octahedral complex with Fe^{II}.[35] A shorter metal-metal distance requires a different macrocycle design.

(d) Region IV

Two changes were made in the M binding site of the reference molecule by replacement of the triamine chain with macrocyclic components. The 1,3-phenylene connectors were retained in both cases. The 7-Me-[12]aneSN_3 ring was appended by the procedure of Figure 3 to give macrocycle **5** with a 22-membered internal ring. The unsubstituted [12]aneSN_3 ring has been prepared and binds divalent ions including Cu^{II} and Zn^{II} with three M-N bonds and a longer M-S interaction.[36] The macrocycle readily forms pincer hydroxo complex **21** (50%) from which **22-25** (40-60%) are prepared as indicated in Figure 12. Structures of the macrocycle and these complexes are collected in Figure13. NH_4HCO_3acts as a proton donor to **21**, yielding aquo complex **22** whose Ni-O bond is 0.10 Å longer than **21**; **22** should be reactive to substitution at the Ni^{II} site. Two equiv of $FeCl_2$ results in unexpected removal of the hydroxo group for chloride and insertion of Fe^{II} in the SN_3 site to afford the unbridged complex **23** with a TBP iron site ($\tau = 0.91$). Cyano-bridged Ni/Fe complex **24** results from hydroxo substitution of **21**. It features a bridge more closely approaching linearity than **19** and a six-coordinate iron site with a weak Fe-S interaction (2.528(1) Å). Hydroxo-bridged Ni/Cu complex **25** is readily formed by the reaction of Cu^{II} with **21** and contains a non-planar CuN_2OS site with one nitrogen atom uncoordinated. These results reveal that macrocycle **5** can stabilize binuclear unbridged and hydroxo- and cyano-bridged complexes with variable coordination at the M site. This structural design should be capable of elaboration with other macrocycles as the M site. One closely related example is 1,7-Me_2/[12]aneN_4[37] (1,7-Me_2-cyclen), which binds divalent metal ions with high affinity.[38] Another example is considered next.

The procedure in Figure 4, which involves reaction of the benzylic bromide **6a** with the substituted cyclam 1,8-Me_2-[14]aneN_4, deprotection of **6b** with hydrazine, and coupling of **6c** with pyridine-2,6-dicarbonylchloride, affords macrocycle **6** with the substituted cyclam ring as the M site. Reactions of **6** are summarized in Figure 14 and the structure of the macrocycle and its complexes are presented in Figure 15. Reaction of **6** with $Ni(OTf)_2$ leads

to mononuclear **26** (46%) whose coordination unit is isostructural with **13, 17**, and **21**. Reaction with Cu^{II} affords the bis(DMF) hydroxo-bridged complex **27** (80%) which upon recrystallization from a solvent mixture containing a small amount of DMF converts to the mono-DMF adduct **28**.[14] Bridge dimensions of the two complexes are quite similar (Table 1).

Complex **27** contains two unexpected features. The Ni^{II} site is six-coordinate with *trans* DMF ligands (O-Ni-O = 177.7(2)E) and bond lengths (2.14-2.15 Å) *ca.* 0.10-0.15 Å longer than in (paramagnetic) $[Ni(DMF)_6]^{2+}$ (Ni-O = 2.04-2.06 Å)[39,40] and various cationic pincer complexes (unreported magnetism).[41-43] In **28** this distance decreases to 2.052(4) Å in the absence of a *trans* ligand.[43] All Ni^{II}-OH complexes in DMF solution show ^{1}H NMR spectra indicative of diamagnetism and weak or nil out-of-plane coordination. We have not encountered additional ligation in any other Ni^{II} NNN pincer coordination unit where the strong in-plane ligand field is expected to favor a planar structure. However, compared to diamagnetic **26**, the Ni-N bond lengths in **27** and **28** are 0.16-0.25 Å and Ni-OH bond lengths are 0.19-0.24 Å longer (Figure 15, Table 1). These results imply a spin state change at Ni^{II} to $S = 1$ (as in $[Ni(DMF)_6]^{2+}$) upon DMF binding.

The Cu^{II} atom in **27** and **28** does not assume CuN_4 binding in the cyclam ring but instead assumes an irregular four-coordinate CuN_3O structure with N4 uncoordinated at 3.07 Å; bonded Cu-N distances are 2.07-2.08 Å. Similar distorted stereochemistry occurs at the Cu^{II} sites in **18**, **25**, and **28**. Given the binding affinity of cyclam-type ligands toward Cu^{II}, and the occurrence of the planar CuN_4 unit in such complexes,[44-46] we conclude that the macrocycle conformation does not favor this conventional coordination mode. A similar factor apparently is operative in **25** as well. Nonetheless, Cu^{II} is bound tightly in these structures.

Bridge Structures

Macrocyclic binucleating ligands facilitate entry to and sustain the viability of supported $[Ni^{II}\text{-}X\text{-}M^{II}]$ bridges with $X = OH^-$ and CN^- and variable M. Whereas homometallic hydroxo and cyano bridges between divalent ions are commonplace, supported or unsupported heterometallic bridges—especially one such bridge per molecule—are not. Such bridges nearly always require one trivalent ion, as exemplified by, *e.g.*, the assemblies $[Fe^{III}\text{-}(OH)\text{-}Cu^{II}]$[47] and $[Fe^{III}\text{-}(CN)\text{-}Cu^{II,I}]$[46,48,49] prepared in this laboratory. We examine briefly the metric features collected in Table 1.

In the mononuclear diamagnetic Ni^{II}-OH complexes **13**, **17**, **21**, and **26**, Ni-O bond lengths are nearly constant at 1.802(4)-1.825(2) Å. Hydroxo-bridged complexes **14-16**, **18**, and **25** when compared against the appropriate member of this set show Ni-O bond length increases of 0.06-0.10 Å indicative of diamagnetic Ni^{II}. With **27** and **28**, increases are larger (0.19, 0.24 Å) because of apparent high-spin Ni^{II} in these complexes. Increases in Ni-O bond lengths are to be expected upon bridge formation and are relatively small with diamagnetic Ni^{II}. Hydroxo bridges of **14-18** exhibit small variations in Ni-O-M angles (140-147E) and Ni···M distances (3.70-3.87 Å). The shortest distance is associated with the near-TBP Cu^{II} stereochemistry in **16**, and the longest with the unexpected four-coordinate Cu^{II} site in **18**. The structures in Figures 8 and 10 and the data of Table 1 delineate the $Ni^{II}\text{-}(OH)\text{-}M^{II}$ bridge geometry supported by macrocycles **2** and **3** for metal ionic radii of 0.7-0.9 Å. Figures 13 and 15, and Table 1 convey this information for complexes derived from macrocycles **5** and **6**.

Cyano-bridged complexes **19** and **24**, based on different macrocycles **3** and **5**, respectively, reveal Ni-C bonds that differ by 0.04 Å, expected nearly linear Ni-C-N fragments (170E), and bent Fe-N-C segments whose angles (138E, 157E) are presumably dependent on

macrocyclic constraints. These results together with the structure of [Ni(CN)FeCl(⊂$_{22}$-pyN_2dien^{Me3})][7] show that **2**, **3**, and **5** are capable of supporting two-atom bridges, here at Ni···Fe distances of 4.71 and 4.93 Å. Lastly, unbridged **23** with two oppositely placed chloride atoms in the bridging void, exhibits a Ni···Fe distance of 5.315(1) Å, the best current measure of the maximum distance available for insertion of a bridging group in macrocycle **5**. No such complex has been isolated with the other macrocycles.

Supplementary Material

Refer to Web version on PubMed Central for supplementary material.

Acknowledgments

This research was supported by NIH Grant GM 28856. We thank Dr. Shao-Liang Zheng for crystallographic assistance and useful discussions. ChemMetCARS Sector 15 at the APS is principally supported by the National Science Foundation-Department of Energy under grant number NSF-CHE-0822838. Use of the APS was supported by the U. S. Department of Energy, Office of Science, Office of Basic Energy Sciences, under Contract No. DE-AC02-06CH11357.

REFERENCES

1. Jeoung J/H, Dobbek H. Science. 2007; 318:1461–1464. [PubMed: 18048691]
2. Gong W, Hao B, Wei Z, Ferguson DJ, Tallant T, Krzycki JA, Chan MK. Proc. Natl. Acad. Sci. USA. 2008; 105:9558–9563. [PubMed: 18621675]
3. Kung Y, Doukov TI, Seravalli J, Ragsdale SW, Drennan CL. Biochemistry. 2009; 48:7432–7440. [PubMed: 19583207]
4. Amara P, Mouesca J/M, Volbeda A, Fontecilla/Camps JC. Inorg. Chem. 2011; 50:1868–1878. [PubMed: 21247090]
5. Panda R, Berlinguette CP, Zhang Y, Holm RH. J. Am. Chem. Soc. 2005; 127:11092–11101. [PubMed: 16076217]
6. Sun J, Tessier C, Holm RH. Inorg. Chem. 2007; 46:2691–2699. [PubMed: 17346040]
7. Huang D, Holm RH. J. Am. Chem. Soc. 2010; 132:4693–4701. [PubMed: 20218565]
8. Abbreviations are given in Chart 1.
9. Huang D, Makhlynets OV, Tan LL, Lee SC, Rybak/Akimova EV, Holm RH. Proc. Natl. Acad. Sci. USA. 2011; 108:1222–1227. [PubMed: 21220298]
10. Huang D, Makhlynets OV, Tan LL, Lee SC, Rybak-Akimova EV, Holm RH. Inorg. Chem. 2011; 50:10070–10081. [PubMed: 21905646]
11. Vigato PA, Tamburini S, Bertolo L. Coord. Chem. Rev. 2007; 251:1311–1492.
12. Vigato PA, Tamburini S. Coord. Chem. Rev. 2008; 252:1871–1995.
13. Vigato PA, Peruzzo V, Tamburini S. Coord. Chem. Rev. 2012; 256:953–1114.
14. See paragraph at the end of this article for Supporting Information available.
15. Coulter KR, McAuley A, Rettig S. Can. J. Chem. 2001; 79:930–937.
16. Brown FJ, Bernstein PR, Cronk LA, Dosset DL, Hebbel KC, Maduskuie TP Jr. Shapiro HS, Vacek EP, Yee YK, Willard AK, Krell RD, Snyder DW. J. Med. Chem. 1989; 32:807–826. [PubMed: 2704027]
17. Rensing S, Schrader T. Org. Lett. 2002; 2:2161–2164. [PubMed: 12074657]
18. dos Santos JL, Lanaro C, Lima LM, Gambero S, Franco-Penteado CF, Alexandre-Moreira S, Wade M, Yerigenhally S, Kutlar A, Meiler SE, Costa FF, Chung M. J. Med. Chem. 2011; 54:5811–5819. [PubMed: 21766854]
19. (a) Harata M, Hasegawa K, Jitsukawa K, Masuda H, Einaga H. Bull. Chem. Soc. Jpn. 1998; 71:1031–1038.(b) Fujisawa K, Kobayashi T, Fujita K, Kitajima N, Moro/oka Y, Miyshita Y, Yamada Y, Okamoto K. Bull. Chem. Soc. Jpn. 2000; 73:1797–1804.(c) Berreau LM, Mahapatra S, Halfen JA, Young VG Jr. Tolman WB. Inorg. Chem. 1996; 35:6398–6341.(d) Jitsukawa K, Harata M, Arii H, Sakurai H, Masuda H. Inorg. Chim. Acta. 2001; 324:108–116.(e) Tubbs KJ, Fuller AL,

Bennett B, Arif H, Berreau LM. Inorg. Chem. 2003; 42:4790–4791. [PubMed: 12895095] (f) Price JR, Fainerman-Melnikova M, Fenton RR, Gloe K, Lindoy LF, Rambusch T, Skelton BW, Turner P, White AH, Wichmann K. Dalton Trans. 2004:3715–3726. [PubMed: 15510298] (g) Cheruzel LE, Cecil MR, Edison SE, Mashuta MS, Baldwin MJ, Buchanan RM. Inorg. Chem. 2006; 45:3191–3202. [PubMed: 16602775] (h) Yao L, Li W-H. Acta Crystallogr. 2009; E65:m1532.(i) Huang M-L. Acta Crystallogr. 2010; E66:m1312.(j) Yoshida Y, Miyamoto R, Nakato A, Santo R, Kuwamura N, Gobo K, Nishioka T, Hirotsu M, Ichimura A, Hashimoto H, Kinoshita I. Bull. Chem. Soc. Jpn. 2011; 64:600–611.

20. Lee SC, Holm RH. J. Am. Chem. Soc. 1993; 115:11789–11798.
21. Donoghue PJ, Tehranchi J, Cramer CJ, Sarangi R, Solomon EI, Tolman WB. J. Am. Chem. Soc. 2011; 133:17602–17605. [PubMed: 22004091]
22. Kitajima N, Hikuchi S, Tanaka M, Moro-oka Y. J. Am. Chem. Soc. 1993; 115:5496–5508.
23. Bazzicalupi C, Bencini A, Bencini A, Bianchi A, Corana F, Fusi V, Giorgi C, Paoli P, Paoletti P, Valtancoli B, Zanchini C. Inorg. Chem. 1996; 35:5540–5548. [PubMed: 11666744]
24. Nishida Y, Yatani A, Nakao Y, Taka J, Kashino S, Mori W, Suzuki S. Chem. Lett. 1999:135–136.
25. Fenandes C, Neves A, Bortoluzzi AJ, Szpoganicz B, Schwingel E. Inorg. Chem. Commun. 2001; 4:354–357.
26. Jones PG, Hrib CG, Petrovic D, Tamm M. Acta Crystallogr. 2007; E63:m2768.
27. Petrovic D, Bannenberg T, Randoll S, Jones PG, Tamm M. Dalton Trans. 2007:2812–2822. [PubMed: 17592598]
28. Wasilke J-C, Wu G, Bu X, Kehr G, Erker G. Organometallics. 2005; 24:4289–4297.
29. Dwyer AN, Grossel MC, Horton PN. Supramol. Chem. 2004; 16:405–410.
30. Wallenhorst C, Axenov KV, Kehr G, Samec JSM, Fröhlich R, Erker GZ. Naturforsch. 2007; 62b: 783–790.
31. Tyler LA, Olmstead MM, Mascharak PK. Inorg. Chim. Acta. 2001; 321:135–141.
32. Harrop TC, Tyler LA, Olmstead MM, Mascharak PK. Eur. J. Inorg. Chem. 2003:475–481.
33. Addison AW, Nageswara Rao T, Reedijk J, van Rijn J, Verschoor GC. J. Chem. Soc., Dalton Trans. 1984:1349–1356.
34. Jeoung J-H, Dobbek H. J. Am. Chem. Soc. 2009; 131:9922–9923. [PubMed: 19583208]
35. Brooker S, Simpson TJ. J. Chem. Soc., Dalton Trans. 1998:1151–1154.
36. Marcus ST, Bernhardt PV, Grondahl L, Gahan LR. Polyhedron. 1999; 18:3451–3460.
37. Piersanti G, Varrese MA, Fusi V, Giorgi L, Zappia G. Tetr. Lett. 2010; 51:3436–3438.
38. Ciampolini M, Micheloni M, Nardi N, Paoletti P, Dapporto P, Zanobini F. J. Chem. Soc., Dalton Trans. 1984:1357–1362.
39. Li W-S, Blake AJ, Champness NR, Schröder M, Bruce DW. Acta Crystallogr. 2012; C54:349–351.
40. McKee V, Metcalfe T, Wikaira J. Acta Crystallogr. 1996; C52:1139–1141.
41. Behrens H, Fröhlich R, Würthwein E-U. Eur. J. Org. Chem. 2005:3891–3899.
42. Chen X, Zhang L, Yu J, Hao X, Liu H, Sun W-H. Inorg. Chim. Acta. 2011; 370:156–163.
43. Huang D, Deng L, Sun J, Holm RH. Inorg. Chem. 2009; 48:6159–6166. [PubMed: 19459662]
44. Tasker PA, Sklar LJ. Cryst. Mol. Struct. 1975; 5:329–344.
45. Elias H. Coord. Chem. Rev. 1999; 187:37–73.
46. Scott MJ, Holm RH. J. Am. Chem. Soc. 1994; 116:11357–11367.
47. Scott MJ, Zhang HH, Lee SC, Hedman B, Hodgson KO, Holm RH. J. Am. Chem. Soc. 1995; 117:568–569.
48. Scott MJ, Lee SC, Holm RH. Inorg. Chem. 1994; 33:4651–4662.
49. Lim BS, Holm RH. Inorg. Chem. 1998; 37:4898–4908. [PubMed: 11670655]

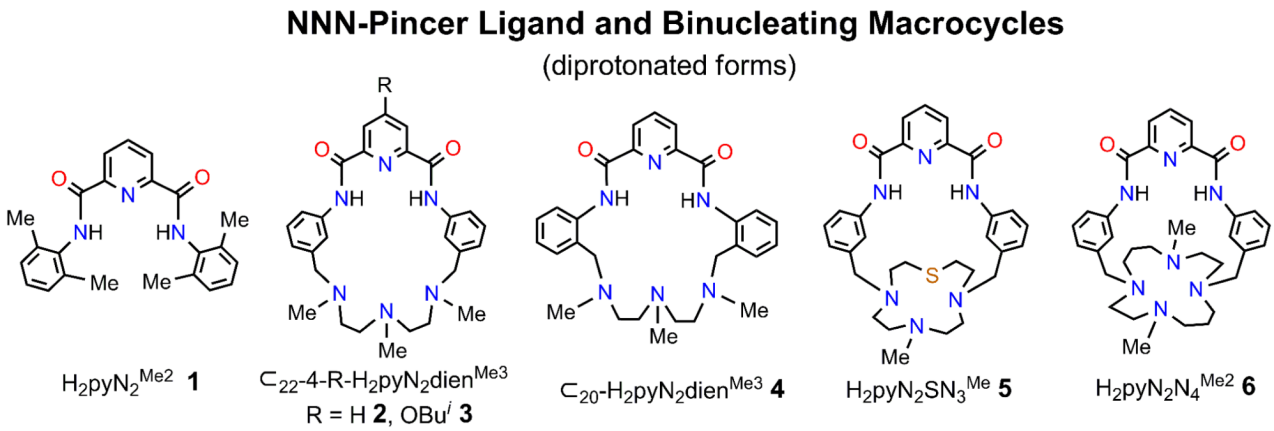

Figure 1.

Depictions of NNN-pincer ligand **1** and binucleating macrocycles **2-6** with ligand abbreviations. The subscript to the symbol ⊂ refers to the number of atoms in the macrocyclic ring.

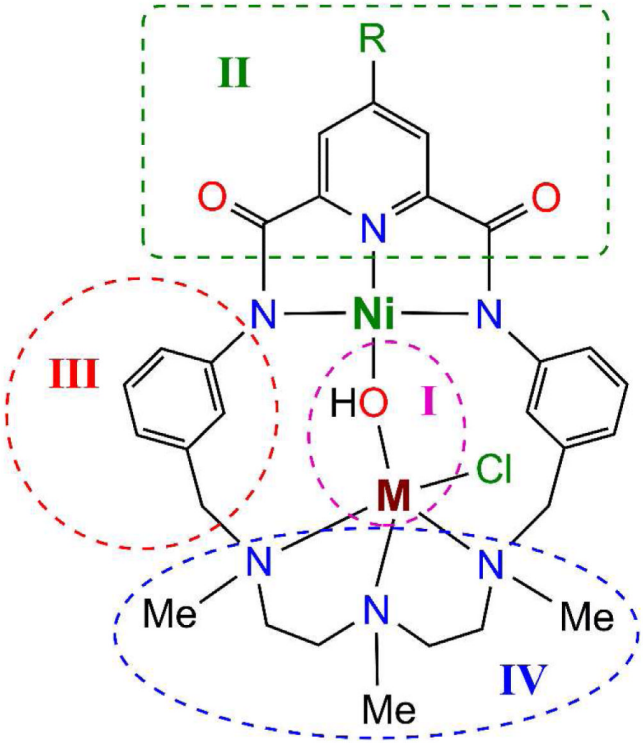

Figure 2.
The binuclear complex [Ni(OH)ML($\subset_{22}$-pyN_2dien^{Me3})] with regions I-IV designated for possible structural alteration.

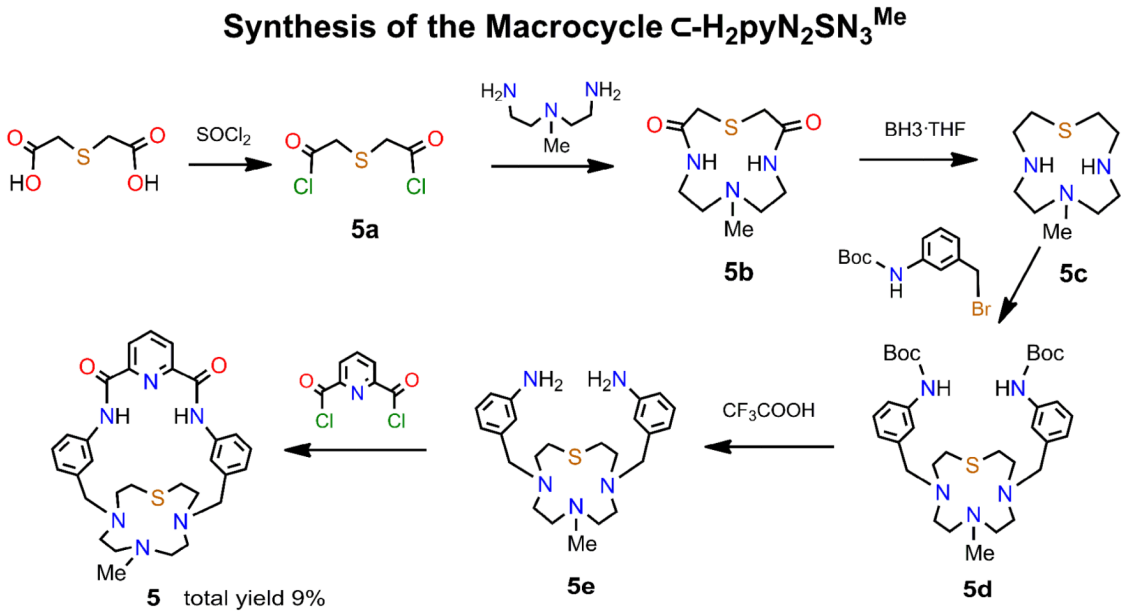

Figure 3.
Synthetic scheme for macrocycle **5** via intermediates **5a-5e**.

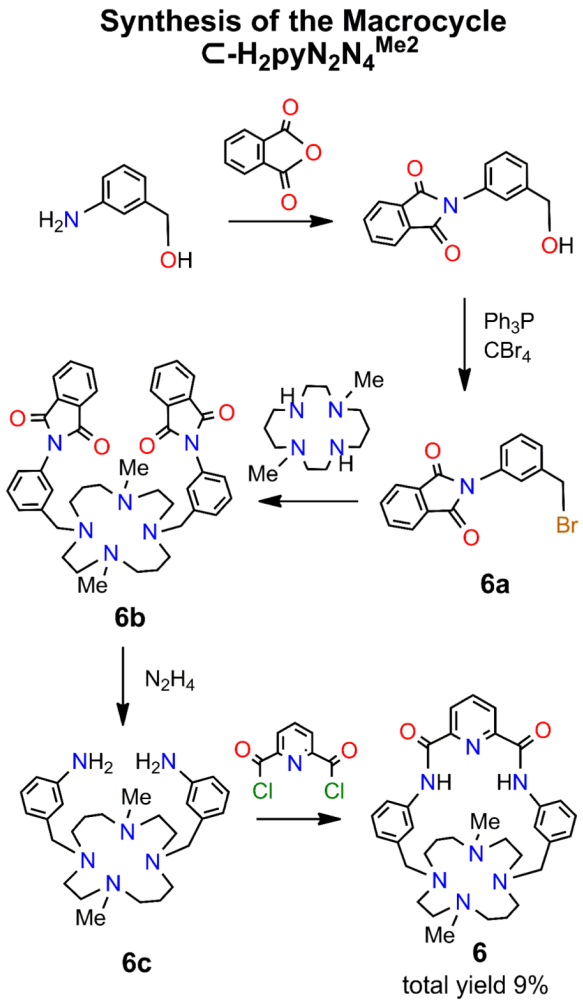

Figure 4.
Synthesic scheme for macrocycle **6** via intermediates **6a-6c**.

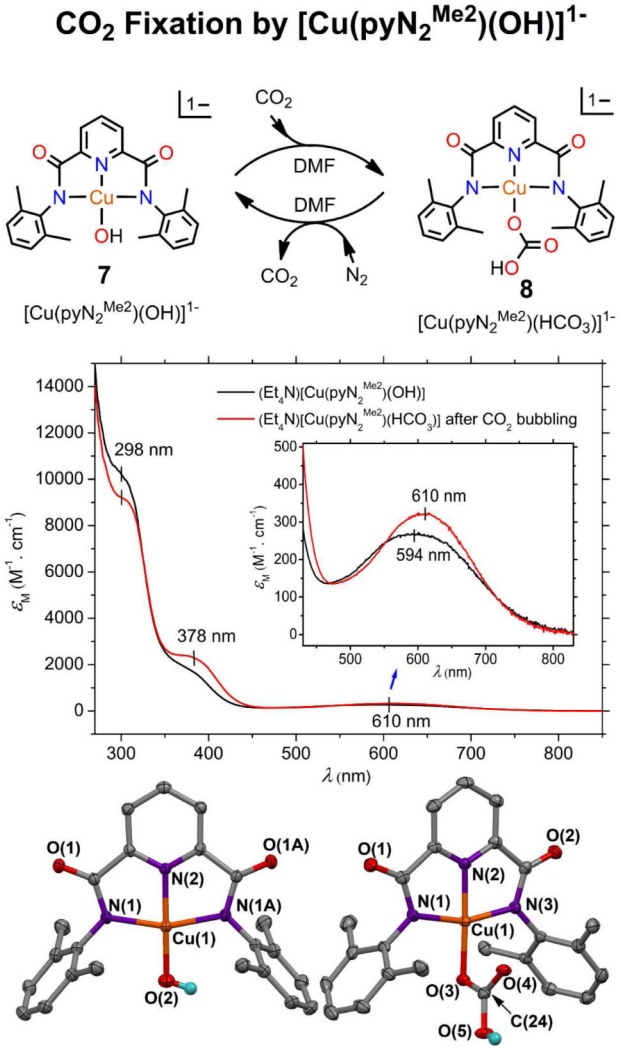

Figure 5.

UV-visible spectrum of the reaction of carbon dioxide with $[Cu(pyN_2^{Me2}{}_2)(OH)]^{1-}$ after 15 min bubbling in DMF solution at room temperature and the structures of the reactant and product complexes. Selected bond distances (Å) and angles (deg): $[Cu(pyN_2^{Me2}{}_2)(OH)]^{1-}$ Cu-O(2) 1.845(3), Cu-N(1) 2.004(2), Cu-N(2) 1.924, N(1)-Cu-N(2) 80.01(6), N(2)-Cu-O(2) 175.5(1); $[Cu(pyN_2^{Me2})(HCO_3)]^{1-}$ Cu-O(3) 1.946(2), Cu-N(1) 2.005(3), Cu-N(2) 1.912(3), Cu-N(3) 1.996(2), Cu···O(4) 2.542(3), N(2)-Cu-O(3) 178.0(1). In this and succeeding X-ray structures, 50% probability ellipsoids are depicted.

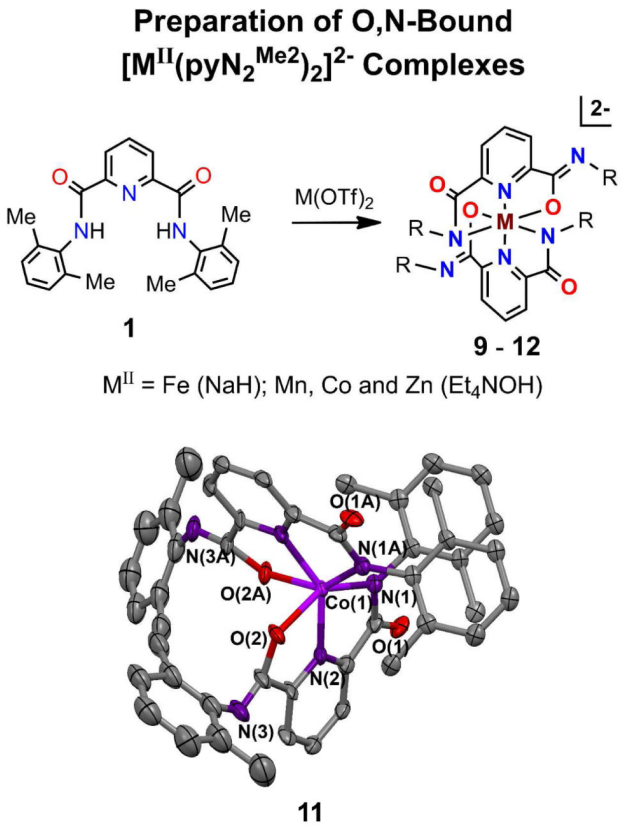

Figure 6.

Preparation of a set of O,N-bound complexes $[M^{II}(pyN_2^{Me2}{}_2)]^{2-}$ (M = Mn, Fe, Co, Zn); ligand deprotonation reagents are indicated. The structure of $[Co^{II}(pyN_2^{Me2}{}_2)]^{2-}$ is shown with the atom labeling scheme. A crystallographically imposed C_2 axis relates atoms X(n) and X(nA). Selected bond distances (Å) and angles (deg): Co-N(1) 2.134(3), Co-N(2) 2.028(3), Co-O(2) 2.226(2), N(1)-Co-N(2) 77.1(1), N(2)-Co-O(2) 74.3(1), O(2)-Co-O(2A) 96.4(1), N(2)-Co-N(2A) 145.6(2), O(2)-Co-N(1) 149.4(1), N(2)-Co-N(1A) 127.1(1). Other angles at the Co atom are in the 83-98E range.

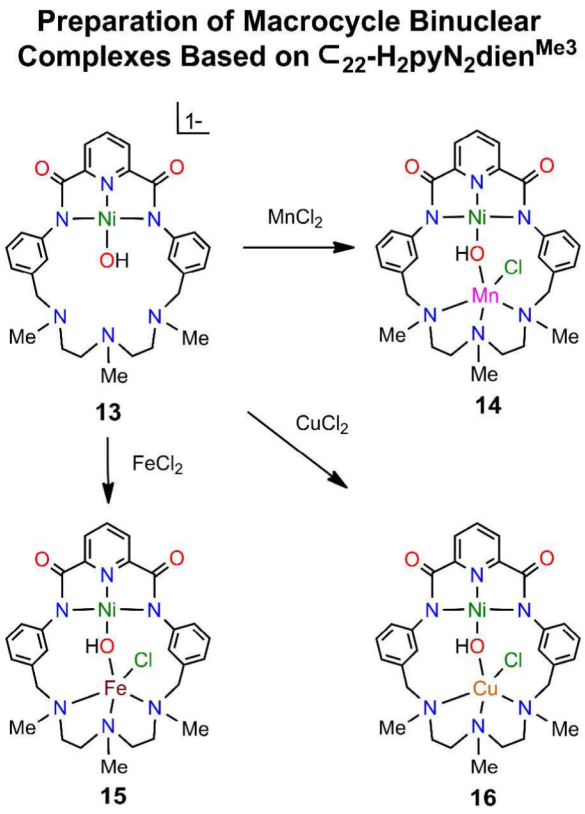

Figure 7.
Formation of binuclear hydroxo-bridged complexes **14-16** from Ni^{II}-OH complex **13** based on macrocycle **2**.

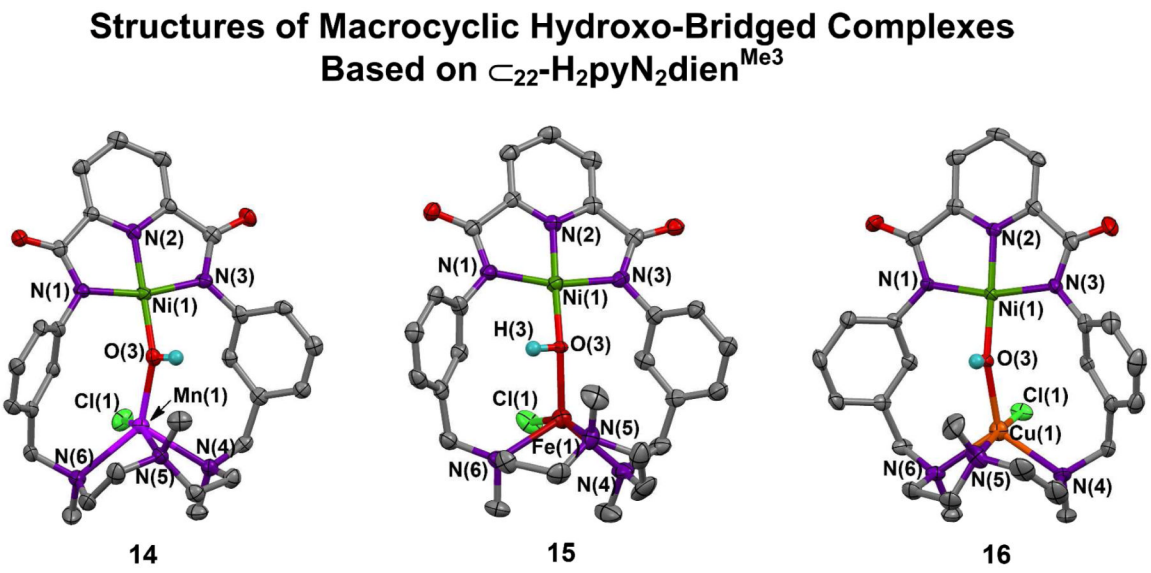

Figure 8.
Structures of complexes containing the Ni^{II}-OH-M^{II} bridge unit (M^{II} = Mn (**14**), Fe (**15**), Cu (**16**)). Complex **15**[7] is included for comparison.

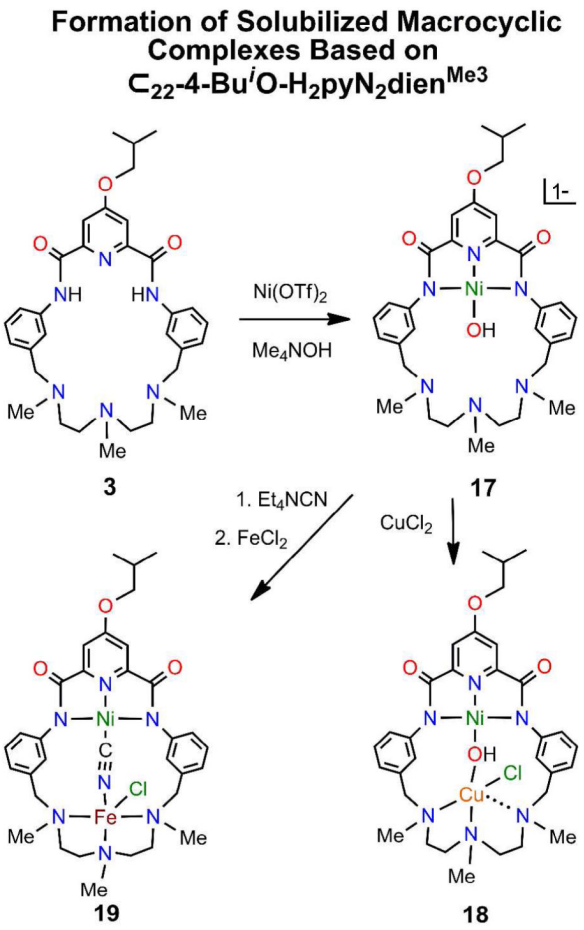

Figure 9.
Formation of solubilized binuclear bridged complexes **18** and **19** from Ni^{II}-OH complex **17** based on macrocycle **3**.

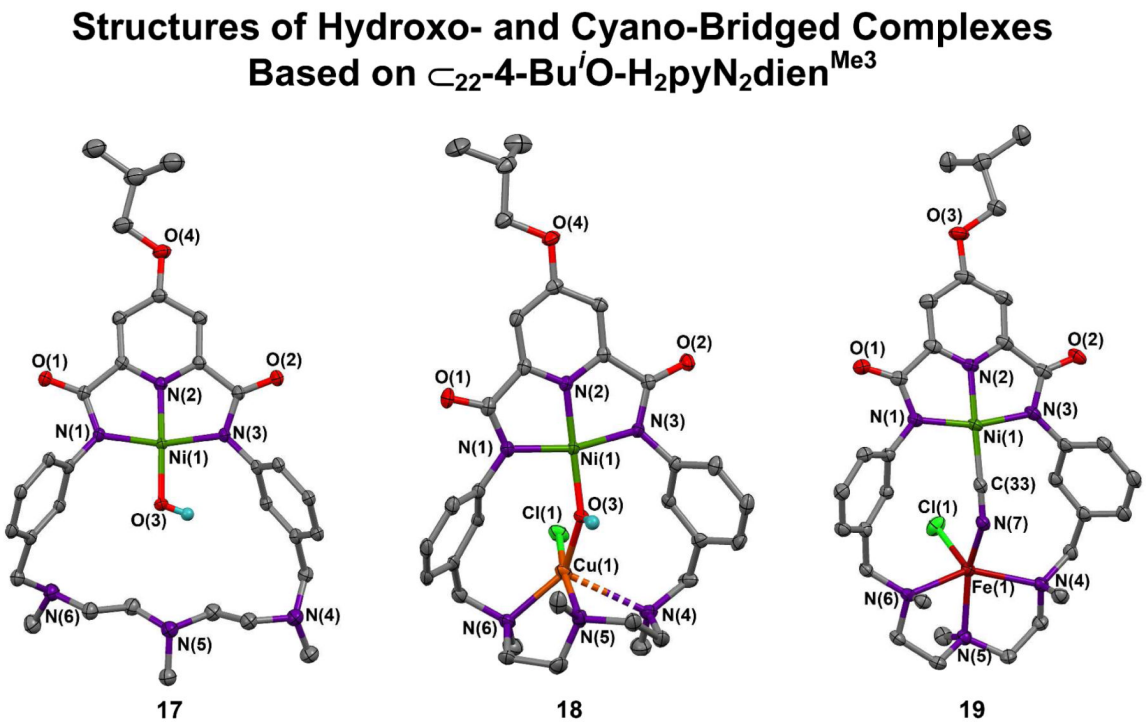

Figure 10.

Structures of Ni^{II}-OH complex **17** and binuclear complexes containing the bridge units Ni^{II}-OH-Cu^{II} (**18**) and Ni^{II}-CN-Fe^{II} (**19**). Ni-N_3 site of **17**: Ni-N(1) 1.912(2) Å, Ni-N(3) 1.916(2) Å, Ni-N(2) 1.828(2) Å, N(1)-Ni-N(2) 82.5(1)E, N(2)-Ni-N(3) 82.2(1)E, N(1)-Ni-N(3) 163.8(1)E. Cu site of **18**: Cu-N(5) 2.033(3) Å, Cu-N(6) 2.130(3) Å, Cu-Cl(1) 2.239(1) Å, Cu···N(4) 2.702(3) Å.

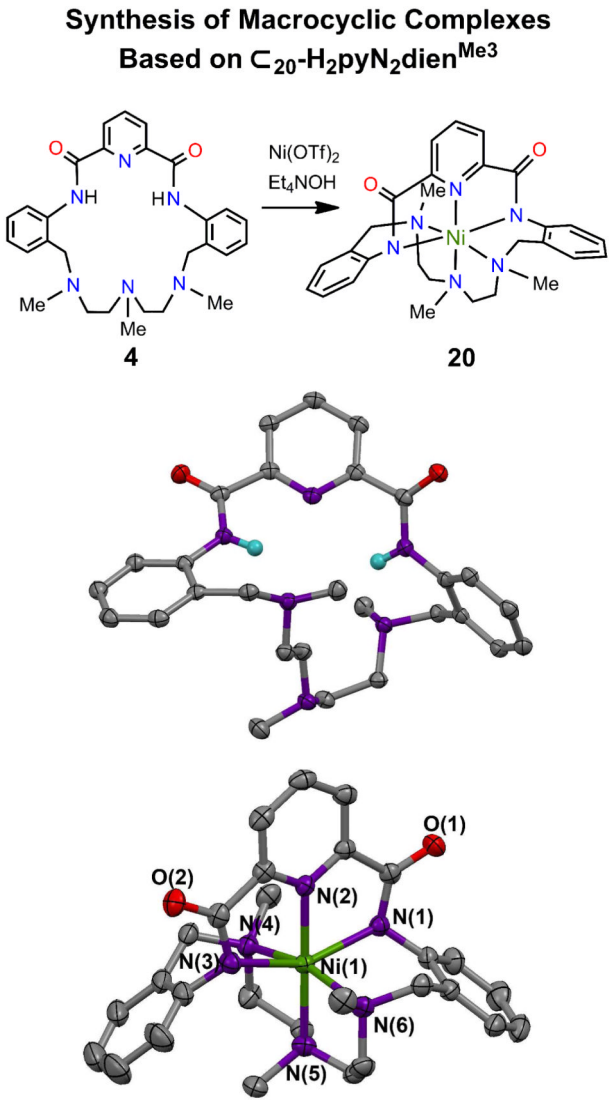

Figure 11.
Formation of the Ni^{II} complex **20** derived from macrocycle **4** and the structures of the macrocycle and the complex.

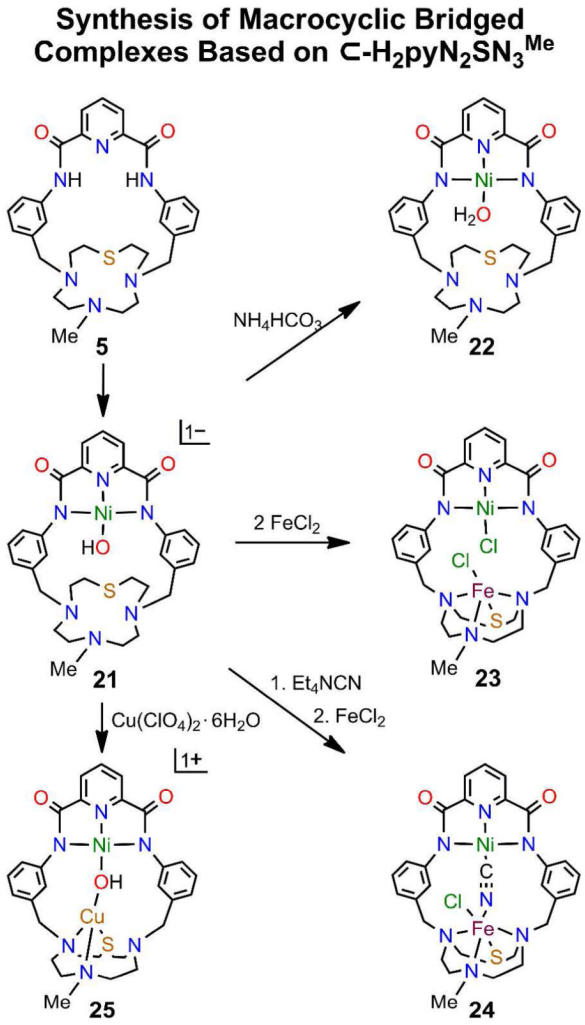

Figure 12.

Formation of mononuclear Ni^{II}-OH complex **21**, aquo complex **22**, unbridged binuclear Ni-Fe complex **23**, and bridged binuclear complexes **24** and **25** based on macrocycle **5**.

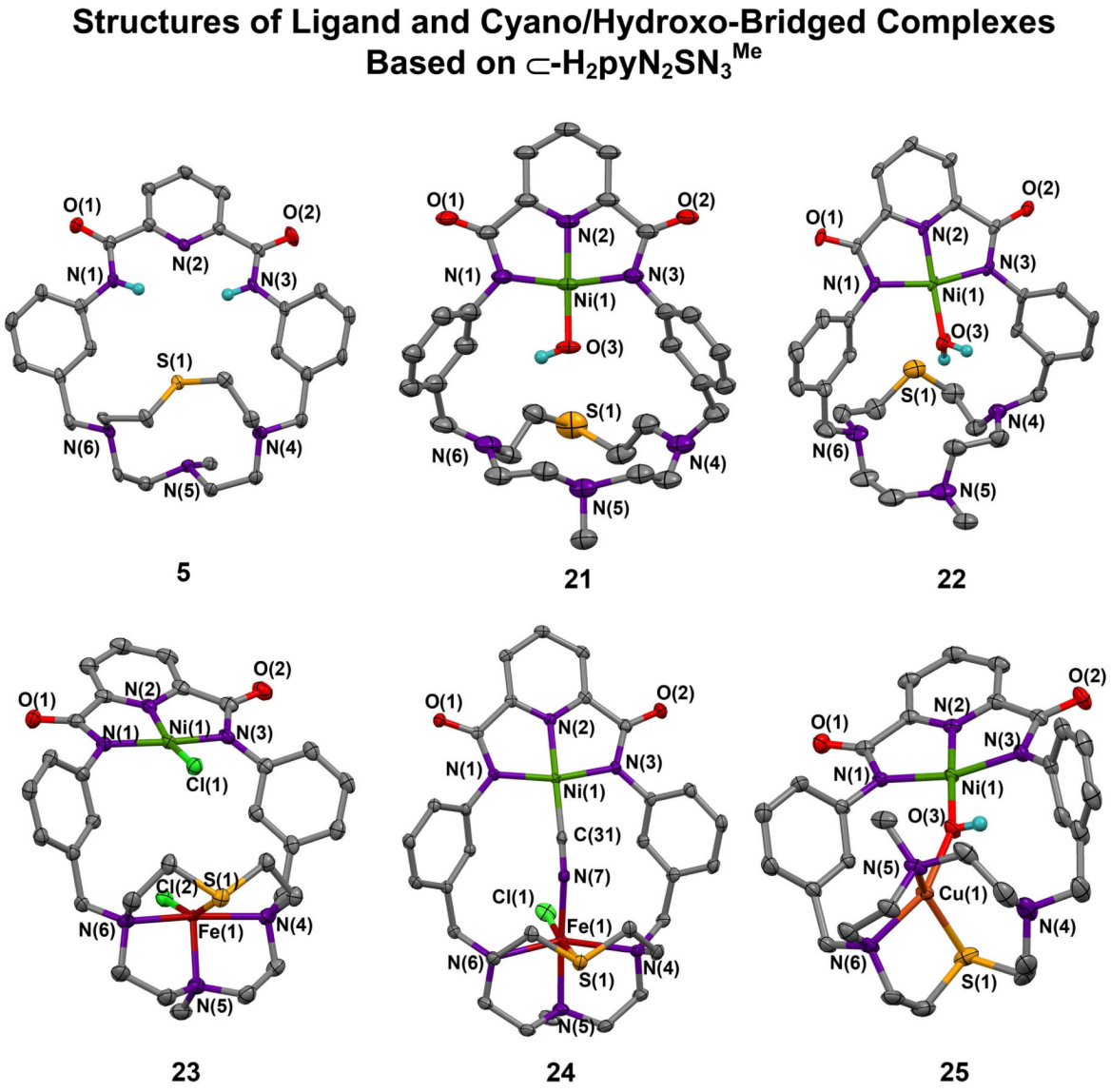

Figure 13.

Structures of macrocycle **5**, mononuclear Ni^{II} complexes **21** (Ni-O 1.824(4) Å) and **22** (Ni-O 1.917(2) Å) derived from **5**, unbridged **23**, and bridged reaction products **24** and **25** from **21**. Fe site in **24** (Å): Fe-Cl(1) 2.342(1), Fe-N 2.084(3)-2.339(2), Fe-S 2.528(1). Cu site in **25** (Å): Cu-N(5) 2.018(4), Cu-N(6) 2.037(3), Cu-S(1) 2.358(1), Cu···N(4) 3.011(4).

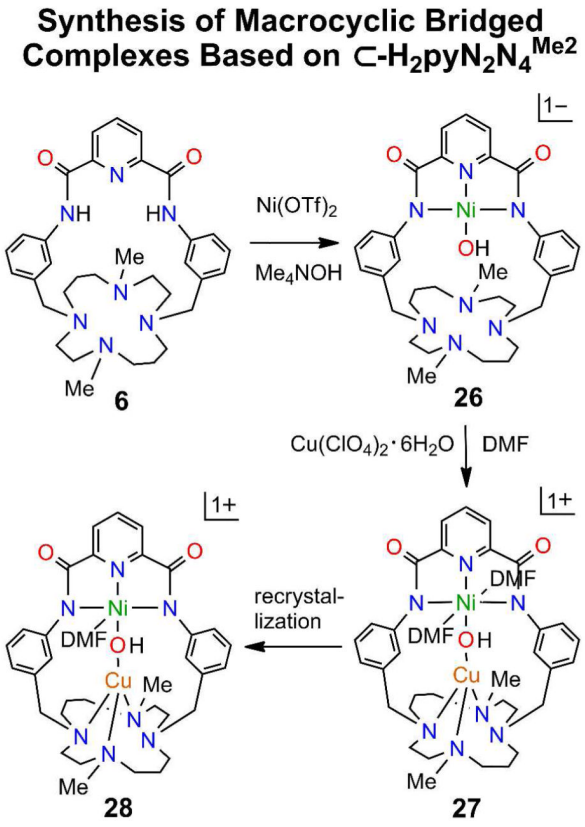

Figure 14.
Formation of mononuclear Ni^{II}-hydroxo complex **26** and binuclear hydroxo-bridged complexes **27** and **28** based on macrocycle **6**.

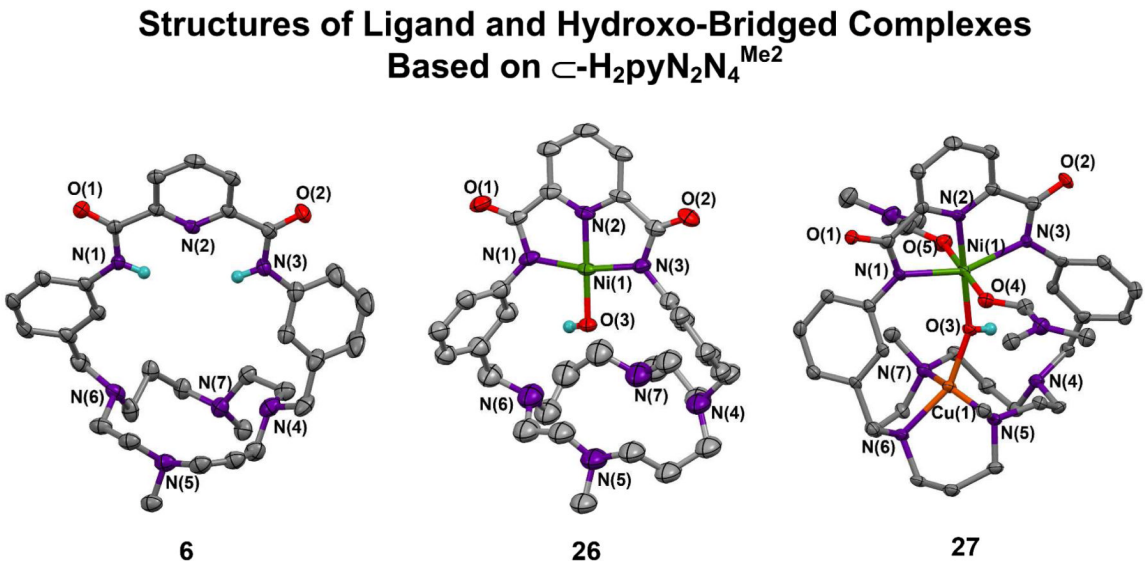

Figure 15.

Structures of macrocycle **6**, mononuclear Ni^{II}-OH complex **26**, and binuclear complex **27** containing a Ni^{II}-OH-Cu^{II} bridge. Ni site in **26** (Å): Ni-N(1) 1.917(9), Ni-N(2) 1.828(3), Ni-N(3) 1.902(8), Ni-O(3) 1.821(2). Ni site in **27** (Å): Ni-N(1) 2.110(4), Ni-N(2) 1.991(4), Ni-N(3) 2.149(4). Cu site in **27** (Å): Cu-N(5) 2.073(4), Cu-N(6) 2.084(4), Cu-N(7) 2.067(5), Cu···N(4) 3.070(4).

$H_2pyN_2^{Me2}$	**1**
$\subset_{22}$-$H_2pyN_2dien^{Me3}$	**2**[7]
$\subset_{22}$-4-Bu^{i}O-$H_2pyN_2dien^{Me3}$	**3**
$\subset_{20}$-$H_2pyN_2dien^{Me3}$	**4**
$\subset$-$H_2pyN_2SN_3^{Me}$	**5**
$\subset$-$H_2pyN_2N_4^{Me2}$	**6**
$[Cu(pyN_2^{Me2})L]^{1-}$	L = OH^- **7**, HCO_3^- **8**
$[M(pyN_2^{Me2})_2]^{2-}$	M^{II} = Mn **9**, Fe **10**, Co **11**, Zn **12**
$Ni(OH)(\subset_{22}$-$pyN_2dien^{Me3})]^{1-}$	**13**[7]
$[Ni(\mu_2$-OH)$MCl(\subset_{22}$-$pyN_2dien^{Me3})]$	M^{II} = Mn **14**, Fe[7] **15**, Cu **16**,
$[Ni(OH)(\subset_{22}$-4-Bu^{i}O-$pyN_2dien^{Me3})]^{1-}$	**17**
$[Ni(\mu_2$-OH)$CuCl(\subset_{22}$-4-Bu^{i}O-$pyN_2dien^{Me3})]$	**18**
$[Ni(\mu_2$-CN)$FeCl(\subset_{22}$-4-Bu^{i}O-$pyN_2dien^{Me3})]$	**19**
$[Ni(\subset_{20}$-$pyN_2dien^{Me3})]$	**20**
$[Ni(OH)(\subset$-$pyN_2SN_3^{Me})]^{1-}$	**21**
$[Ni(OH_2)(\subset$-$pyN_2SN_3^{Me})]$	**22**
$[NiClFeCl(\subset$-$pyN_2SN_3^{Me})]$	**23**
$[Ni(\mu_2$-CN)$FeCl(\subset$-$pyN_2SN_3^{Me})]$	**24**
$[Ni(\mu_2$-OH)$Cu(\subset$-$pyN_2SN_3^{Me})]^{1+}$	**25**
$[Ni(OH)(\subset$-$pyN_2N_4^{Me2})]^{1-}$	**26**
$[Ni(\mu_2$-OH)$(DMF)_2Cu(\subset$-$pyN_2N_4^{Me2})]^{1+}$	**27**
$[Ni(\mu_2$-OH)(DMF)$Cu(\subset$-$pyN_2N_4^{Me2})]^{1+}$	**28**

*$\subset$ = macrocycle, *n* = number of atoms in the ring; OTf^- = $CF_3SO_3^-$;
pyN_2^{Me2} = *N*,*N*'-bis(2,6-dimethylphenyl)-2,6-pyridinedicarboxamidate(2-);
[12]aneSN_3 = 1-thia-4,7,10-triazacyclododecane;
[14]aneN_4 = 1,4,8,11-tetraazacyclotetradecane.
The cumbersome formal nomenclature of the macrocycles is omitted.

Chart 1. Designation of Ligands and Complexes*

Table 1

Ni-X-M Bridge Matric Parameters

Compounds Ni-X-M	**14 Ni-OH-Mn**	**15**[a] **Ni-OH-Fe**	**16 Ni-OH-Cu**	**18 Ni-OH-Cu**	**19 Ni-CN-Fe**
Ni-O/C/Cl (Å)	1.861(3)	1.927(4)	1.899(3)	1.895(2)	1.878(3)
M-O/N/Cl (Å)	2.089(4)	2.059(3)	2.134(4)	2.026(2)	2.099(2)
Ni-O-M (deg)	142.5(2)	140.0(2)	147.6(2)	141.1(1)	-
Ni-C-N (deg)	-	-	-	-	170.2(2)
Fe-N-C (deg)	-	-	-	-	138.3(2)
Ni···M (Å)	3.741(2)	3.747(2)	3.873(2)	3.697 (1)	4.709(1)
Compounds Ni-X-M	**23** Ni-Cl Cl-Fe	**24** Ni-CN-Fe	**25** Ni-OH-Cu	**27** Ni-OH-Cu	**28** Ni-OH-Cu
Ni-O/C/Cl (Å)	2.178(2)	1.853(3)	1.890(3)	2.056(4)	2.008(3)
M-O/N/Cl (Å)	2.236(2)	2.084(3)	1.936(3)	1.924(4)	1.936(3)
Ni-O-M (deg)	-	-	150.4(2)	153.1(2)	152.7(2)
Ni-C-N (deg)	-	170.5(3)	-	-	-
Fe-N-C (deg)	-	157.2(2)	-	-	-
Ni···M (Å)	5.315(1)	4.927(1)	3.699(1)	3.871(1)	3.833(2)

[a]Ref. 7.